# Intrinsic and Environmental Effects in the Structure and Magnetic Properties of Organic Molecular Magnets: Bis(imino)nitroxide

**Vincenzo Barone,*,† Alessandro Bencini,‡ and Andrea di Matteo†**

*Contribution from the Dipartimento di Chimica, Università di Napoli "Federico II", via Mezzocannone 4, I-80134 Napoli, Italy, and Dipartimento di Chimica, Università di Firenze, via Maragliano 75, 50144 Firenze, Italy*

*Received March 27, 1997. Revised Manuscript Received July 11, 1997*[⊗]

**Abstract:** The structure, conformational behavior, and magnetic coupling constant of a prototypical organic molecular magnet (the bis(imino)nitroxide) have been investigated in vacuo and in solution, combining a recent density functional theory/Hartree−Fock model with a refined continuum description of the solvent. Comparison with previous sophisticated computations for a simplified model shows that our approach provides reliable magnetic couplings for a wide range (0−2000 $cm^{-1}$) of interactions between the radical subunits. The computations performed for the true compound at the experimental conformation show that structural and magnetic parameters are in remarkable agreement with experiment. Solvent effects are negligible concerning the magnetic coupling but modify the conformational behavior leading to an inter-ring torsional angle in better agreement with the experimental value.

## Introduction

The experimental investigation of exchange interactions between magnetic centers both in vacuo and in condensed phases constitutes one of the main research topics in modern chemistry.

For instance, magneto-structural correlations are widely used to interpret the magnetism of solids[1] and to develop synthetic strategies affording compounds with expected magnetic properties. Furthermore, in bioinorganic chemistry, the understanding of the magnetic interactions between metal centers provides information about the coordination environment and gives assessments about the geometry of active sites in enzymes.[2]

In the last few years, a number of magnetic systems containing organic free radicals (such as nitroxide derivatives) and paramegnetic transition metal ions have been synthetized as possible precursors for ferromagnetic materials.[3]

Furthermore, the particular stability of mono- and polynitroxide radicals offers the possibility of synthesizing and studying different molecular systems[4] in which the nitroxide groups can be used as "spin labels" to explore the structure of the chemical environment of the radicals[5] or to provide possible precursors for purely organic magnetic materials.[4] This last aspect has received considerable attention especially after the observation of bulk ferromagnetism in several nitronyl nitroxide radicals and $C_{60}$ charge transfer salts.[6,7]

Organic radicals have two remarkable characteristics, when compared with the conventional transition-metal-based magnetic system. One is the highly isotropic nature of the electron spins as a result of weak spin−orbit coupling in a molecule containing only light elements. Organic radicals are thus suitable for investigating the magnetism of nearly ideal Heisenberg spin systems.

The other characteristic is the distribution of the spin densities on some atoms within a molecule. The spin distribution tunes the magnetic interactions between different units and becomes an important parameter because it can affect even the sign of these interactions.

As a consequence, the computation of reliable spin densities in free radicals is an important prerequisite for any theoretical method developed for the study of magnetic interactions.

At the same time, such unstable species are often difficult to characterize by experimental techniques, since spectroscopic evidences are often only indirectly related to structural parameters. Thus, accurate quantum mechanical methods have been used to provide the link between macroscopic and microscopic characteristics.[8] Unfortunately, the computation of reliable geometrical structures, binding energies, and physicochemical properties of open-shell systems requires theoretical methods including a significant part of electronic correlation. Although the most sophisticated post-Hartree−Fock (HF) methods provide reliable results, they remain prohibitive for molecules containing more than 6 or 7 heavy atoms. Methods rooted in the density functional (DF) theory offer a better compromise between the accuracy of results and the computation time for relatively large systems.[8] Several studies have shown that inclusion of some Hartree−Fock (HF) exchange in gradient−corrected functionals significantly improves their performances leading to accurate structural, thermodynamic, and spectroscopic properties both for closed- and open-shell species.[9] Among these methods, we have selected the so-called B3LYP model obtained combining HF and Becke exchange terms with the Lee−Yang−Parr

* Author to whom correspondence should be addressed at the following: phone +3981-5476503; fax +3981-5527771; e-mail enzo@chemna.dichi.unina.it.

† Università Federico II.

‡ Università di Firenze.

⊗ Abstract published in *Advance ACS Abstracts,* September 1, 1997.

(1) Kahn, O. *Molecular Magnetism*; VCH: New York, 1993.

(2) Bertini, I.; Luchinat, C. *Coord. Chem. Rev.* **1996**, *150*, 1.

(3) (a) Gatteschi, D. *Adv. Mater.* **1990**, *62*, 223. (b) Miller, J. S.; Epstein, A. *Angew. Chem., Int. Ed. Engl.* **1994**, *33*, 385.

(4) Rassat, A. *Pure Appl. Chem.* **1990**, *223*, 62.

(5) Hanson, P.; Lilhauser, G.; Formaggio, F.; Crisma, M.; Toniolo, C. *J. Am. Chem. Soc.* **1996**, *118*, 7618.

(6) Chiarelli, R.; Novak, M. A.; Rassat, A.; Tholince, J. L. *Nature (London)* **1993**, *363*, 147.

(7) Ciujeda, J.; Mas, M.; Molins, E.; Laufranc de Pauthou, F.; Laugier, J.; Park, J. G.; Paulsen, C.; Rey, P.; Rovira, C.; Veciana, J. *J. Chem. Soc., Chem. Commun.* **1995**, 709.

(8) Barone, V. In *Recent Advances in Density Functional Methods*, Part 1; Chong, D. P., Ed.; World Scientific: Singapore, 1995; p 287.

(9) (a) Barone, V. *J. Chem. Phys.* **1994**, *101*, 10666. (b) Adamo, C.; Barone, V.; Fortunelli, A. *J. Chem. Phys.* **1995**, *102*, 384. (c) Barone, V. *Theor. Chim. Acta* **1995**, *91*, 113.

S0002-7863(97)00978-5 CCC: $14.00 

correlation functional in the same ratio as that originally proposed by Becke for a sligthly different combination.[10]

The present paper is devoted in particular to a validation of the B3LYP approach for the study of the structure and properties of large organic magnetic systems. To this end, we consider the structure and spin-dependent properties of the iminonitroxide radical and the conformational and magnetic properties of the biradical obtained by connecting two iminonitroxide rings.

Furthermore, using a recent effective implementation of one of the most reliable continuum solvent models[11] (the so-called polarizable continuum model, PCM), we have also considered possible modifications on the geometric and electronic structure induced by solute−solvent interactions.

This is one of the first applications of the PCM procedure to structural studies of open-shell systems employing DF methods.[11]

The paper is organized as follows. After a short description of computational details, the first section of the results is devoted to the iminonitroxide radical which is stable under ordinary conditions and has been extensively used in the last few years as a molecular brick to design molecular-based magnetic materials.[12,13]

In the second section, we compare the results obtained by multiconfigurational methods of reduced dimension and by the broken symmetry[14] B3LYP formalism to those previously obtained by a refined multiconfigurational approach for a model biradical.

In the third section, we consider a more realistic bis(imino)-nitroxide system closely corresponding to the true biradical studied experimentally except for the replacement of methyl groups by hydrogen atoms. Experimentally, the iminonitroxide rings are not coplanar, but rotated by an angle $\alpha$ of 55°,[15] and this gives an antiferromagnetic exchange interaction placing the singlet state between 163 $cm^{-1}$ (solution data) and 197 $cm^{-1}$ (solid state) below the first excited triplet. We can, therefore, investigate if our approach is able to provide, at the same time, good structural and magnetic properties.

## Theoretical Background

The interaction between magnetic centers is governed by two main factors: the exchange energy between electrons of equal spin, which favors a parallel alignment of the spins between adjacent centers (the so-called potential exchange in the Anderson theory), and the overlap between the magnetic orbitals that favors the antiparallel alignment of the spins (the so-called kinetic exchange in the Anderson theory).[16] As discussed in detail by McConnel and Khan, a reliable description of magnetic interactions can be obtained only considering, together with the above contributions, spin polarization effects.[1,17] Among the methods that take spin polarization into account, the unrestricted Hartree−Fock (UHF) approach has the severe drawback of providing wave functions that are not exact eigenfunctions of the spin operator $\mathbf{S}^2$. For instance, the description of the doublet ground state of simple radicals is contaminated by some contributions of higher spin multiplicities (quartet, sextet, etc.) Some techniques exist that annihilate this contamination, but they are rather difficult to implement and often do not provide a unique solution. A consequence of this contamination is that the spin-unrestricted approach systematically overestimates spin polarization.[18]

In the unrestricted Kohn−Sham (UKS) model, on the contrary, the correlation functional provides a separate estimation of the correlation contribution to energy. There is thus no need to artificially increase the spin polarization of the doubly occupied orbitals. The reliability of the results depends of course on the form of exchange-correlation functional. In particular, Becke has recently emphasized the role of HF exchange in the framework of DF theories and has obtained astonishingly good formation enthalpies optimizing the coefficients of a linear combination of local spin density, gradient corrections, and HF exchange.[10,19] We have shown that a closely related protocol (the so-called B3LYP model) provides good structures, magnetic properties, force fields, and formation enthalpies of open-shell systems.[8,9]

Quantitative calculations of magnetic exchange interactions require an accurate description of the multiplet structure of the molecule for the ground and the lowest excited state.

A model particularly attractive for large systems has been suggested by Noodleman and Norman in 1979,[14] which is based on a broken spin and space symmetry single determinant wave function for describing the low-spin state,[20] accounting for a large part of the electron correlation. Next, a one-to-one correspondence is established between the energy of a Slater determinant built up with orbitals localized on different centers and bearing electrons with opposite spin and the energy of a microstate with $M_S = 0$ computed using the effective Heisenberg−Dirac−VanVleck spin Hamiltonian

$$H = -2\,J\boldsymbol{S}_1\boldsymbol{S}_2 \tag{1}$$

where $J$ is related to the multiplet energy splitting according to

$$E(S_{max}) - E(S = 0) = -S_{max}(S_{max} + 1)J \tag{2}$$

and $E(S_{max})$ represents the energy of a state with total spin $S_{max}$. Equation 1 is widely used to reproduce experimental data, and $J$ is known as the magnetic exchange coupling constant. For a binuclear system of spin $S_1 = S_2$, the energy of the broken symmetry (BS) state is a weighted average of the energies of pure spin multiplets, and $J$ can be obtained through the equation

$$E(S = 1) - E(\mathrm{BS}) = -J \tag{3}$$

where $E$(BS) is the energy of the broken symmetry determinant. The term broken symmetry state is due to the fact that a localized solution of the spin states is usually obtained by using an electronic symmetry lower than the actual geometric symmetry.

Use of eq 3 reduces the calculation of the multiplet structure in a binuclear system to the calculation of the total energies of two Slater determinants, one representing the state with the maximum spin multiplicity and the other a state with $M_S = 0$ built up from wave functions localized onto the different magnetic centers.[21] Using spin projection techniques, it has been shown that $E$(BS) accounts for most of the electronic correlation in the singlet state. The actual form of eq 3 has been shown to be valid when the overlap integrals, $S_{12}$, between the magnetic orbitals is small ($S_{12}^2 \ll 1$), which is likely to be the case for weakly bonded paramagnetic moieties. A more general formula has been derived for any value of $S_{12}$, which shows that eq 3 can lead to overestimation of $J$ values as large as 50% when $S_{12} = 1$.[22] By using eq 3, one is therefore always overestimating value of $J$. Note that, in the BS model, the high spin state is completely uncorrelated and its energy is usually taken from spin-unrestricted calculations.

(10) Becke, A. D. *J. Chem. Phys.* **1993**, *98*, 1372.
(11) (a) Cossi, M.; Barone, V.; Cammi, R.; Tomasi, J. *Chem. Phys. Lett.* **1996**, *255*, 327. (b) Barone, V.; Cossi, M.; Rega, N. *J. Chem. Phys.* **1996**, *105*, 11060.
(12) Caneschi, A.; Gatteschi, D.; Sessoli, R.; Rey, P. *Acc. Chem. Res.* **1989**, *2*, 392.
(13) Caneschi, A.; Gatteschi, D.; Rey, P. *Prog. Inorg. Chem.* **1991**, *39*, 331.
(14) (a) Noodleman, L.; Davidson, E. R. *Chem. Phys.* **1979**, *70*, 4903. (b) Noodleman, L. *J. Chem. Phys.* **1981**, *74*, 5737.
(15) Alies, F.; Luneau, D.; Laugier, J.; Rey, P. *J. Phys. Chem.* **1993**, *97*, 2922.
(16) Anderson, P. W. In *Magnetism*; Rado, G. T., Shul, H., Eds.; Academic Press: New York, 1963; Vol. 1.
(17) McConnel, H. M. *J. Chem. Phys*. **1963**, *36*, 1910.
(18) Chipman, D. M. *Theor. Chim. Acta* **1992,** *82*, 93.
(19) Becke, A. D. *J. Chem. Phys.* **1993**, *98*, 5648.
(20) Hart, J. R.; Rappé, A. K.; Gorum, S. M.; Upton, T. H. *J. Phys. Chem.* **1992**, *96*, 6264.
(21) Noodleman, L.; Case, D. A. *Adv. Inorg. Chem.* **1992**, *38*, 423.
(22) Noodleman, L.; Norman, J. G. *J. Chem. Phys*. **1979**, *70*, 4903.

## Computational Details

All of the computations have been performed using a locally modified version of the *Gaussian 94* package[23] and the standard 6-31G* basis set.[24]

The geometrical parameters of the iminonitroxide radical have been fully optimized at the UB3LYP level following the analytical gradient procedure available in the *Gaussian 94* package, with the only constraint of $C_s$ symmetry.

For the bis(imino)nitroxide system, we have performed calculations at the UB3LYP level, both optimizing the geometries at selected values of the inter-ring dihedral angle (flexible rotor model, FRM) and freezing bond lengths and valence angles to the values used in ref 25 (rigid rotor model, RRM). Using these geometries, the energies of triplet and true singlet states have been computed at the CAS(2,2) level, which should provide a reliable evaluation of exchange and superexchange effects, but completely neglects dynamic correlation.

Solvent effects on the structures and magnetic properties have been evaluated using our recent implementation of the polarizable continuum model (PCM).[11] In continuum solvent models, the molecular solute is embedded in a cavity surrounded by an infinite dielectric. In an attempt to describe the actual molecular shape in a realistic way, the PCM approach employs a cavity formed by interlocking spheres centered on the differents atoms (or functional groups) with radii proportional to van der Waals values (here 1.44, 1.8, 1.8, and 1.68 Å for H, C, N, and O, respectively).

The molecular free energy of solvation can be written

$$\Delta G_{solv} = G_{solv} - E_{vac} \tag{4}$$

where $E_{vac}$ is the energy of the molecule isolated and the free energy ($G_{solv}$) of the molecule in solution is written as a sum of contributions:

$$G_{solv} = G_{es} + G_{cav} + G_{disp} + G_{rep} \tag{5}$$

$G_{cav}$, $G_{disp}$, and $G_{rep}$ are collectively referred to as nonelectrostatic terms describing the energy needed to build the cavity and the energy due to the solute solvent dispersion−repulsion interaction, respectively. They are calculated by classical approaches, described elsewhere.[26]

Since, in the PCM formalism, these terms do not enter the molecular Hamiltonian, they affect the total energy but not the solute electron density.

The contribution $G_{es}$, taking into account the electrostatic solute−solvent interactions, is formally analogous to $E_{vac}$; it is calculated by a self-consistent procedure, in terms of a modified Fock matrix[26]

$$F = F^0 + {}^1/_2(j + y) + X \tag{6}$$

and of a modified nuclear repulsion energy:

$$V_{N,N} = V^0{}_{N,N} + {}^1/_2 U_{N,N} \tag{7}$$

$F^0$ and $V^0{}_{N,N}$ are the Fock matrix and the nuclear energy of the isolated molecule, and the terms $j$, $y$, $X$, and $U_{N,N}$ are calculated in terms of apparent polarization charges, distributed over the surface of the cavity containing the solute, which reproduce the reaction field of the solvent. The electrostatic reaction field affects the solute electronic distribution, through eq 6, and then influences both the energy and the electronic properties of the solute.

## Results and Discussion

**(a) The Iminonitroxide Radical.** As mentioned in the Introduction, we have considered the simplest iminonitroxide radical without any substituent, shown in Figure 1.

The ground electronic state of the iminonitroxide radical has 2A″ symmetry, and the unpaired electron is in an orbital essentially formed by mixing of the $\pi^*$ orbital of N−O and the $\pi$ orbital of the iminic N atom (Figure 2).

In Table 1, experimental geometries[27,28] for two different substituents ($R_6$ = $C_6H_4NO_2$ and $C_6H_5$) are compared with structures issuing from full optimizations of the simplest radical ($R_6$ = H) by different computational models.

All of the bond distances calculated by the UB3LYP approach are close to experimental data. As shown in previous work,[25] reasonable results are obtained also at the UHF level except for the NO bond length, which is very sensitive to basis set extension and to inclusion of correlation energy. In view of several other experimental results, one of the X-ray values (1.248 Å) is probably unreliable, whereas a NO bond length in the correct range (1.26−1.28 Å) can be obtained only by introducing the electronic correlation at the MP2 or higher levels (e.g., 1.277 Å at the UMP2/6-31G* level[25]) or by using gradient-corrected density functionals including some HF exchange (e.g., 1.268 Å at the UB3LYP/6-31G* level).

The bond angles, obtained by the UB3LYP/6-31G* computational model, are close to those obtained at the UHF/6-311G* level and show an error of ≅2% with respect to experimental values.

Atomic spin populations (ASPs) for the iminonitroxide radical have been obtained by single-crystal-polarized neutron diffraction on a derived nitrophenyl.[28] The values reported in Table 2 indicate that most of the spin density is located on the N2, N3, and O7 atoms.

B3LYP calculations of ASPs have been performed using the EPR-II basis set,[8,29] which is derived from the popular Huzinaga−Dunning double-$\zeta$ set augmented by standard polarization functions, uncontracting some functions in the outer core−inner valence region. The contraction coefficients of the resulting basis set have been further optimized by atomic UKS computations.

Computations have been performed in vacuo and in a polar solvent for iminonitroxide and a phenyl derivative of the iminonitroxide radical. Theoretical *ASPs* are generally close to experimental values, except those for the $C_1$ atom, probably due to some residual overstimation of spin polarization effects. Note, however, that this effect is attenuated when a phenyl group is bonded to $C_1$.

The modifications of the ASPs of $N_2$ and $O_7$ atoms in a polar solvent are due to the increased weight of resonance structures

(23) Frisch, M. J.; Trucks, G. W.; Schlegel, H. B.; Gill, P. M. W.; Johnson, B. G.; Robb, M. A.; Cheeseman, J. R.; Keith, T. A.; Petersson, G. A.; Montgomery, J. A.; Raghavachari, K.; Al-Laham, M. A.; Zakrewski, V. G.; Ortiz, J. V.; Foresman, J. B.; Cioslowski, J.; Stefanov, B. B.; Nanayakkara, A.; Challacombe, M.; Peng, C. Y.; Ayala, P. Y.; Chen, W.; Wong, M. W.; Andres, J. L.; Replogle, E. S.; Gomperts, R.; Martin, R. L.; Fox, D. J.; Binkley, J. S.; DeFrees, D. J.; Baker, J.; Stewart, J. P.; Head-Gordon, M.; Gonzalez, C.; Pople, J. A. *Gaussian 94, Revision D.4*; Gaussian, Inc: Pittsburgh, PA, 1996.

(24) Hariharan, P. G.; Pople, J. A. *Theor. Chim. Acta* **1973**, *28*, 213.

(25) Barone, V.; Grand, A.; Luneau, D.; Rey, P.; Minichino, C.; Subra, R. *New J. Chem.* **1993**, *17*, 545.

(26) (a) Cammi, R.; Tomasi, J. *J. Chem. Phys.* **1994**, *101*, 3888. (b) Cossi, M.; Tomasi, J.; Cammi, R. *Int. J. Quantum Chem., Quantum Chem. Symp.* **1995**, *29*, 625.

(27) Luneau, D.; Rey, P.; Laugier, J.; Beloritzky, E.; Cogne, A. *Inorg. Chem.* **1992**, *31*, 578.

(28) Zheludev, A.; Bonnet, M.; Delly, B.; Grand, A.; Luneau, D.; Öhrström, L.; Ressouche, E.; Rey, P.; Schweizer J. *J. Magn. Magn. Mater.* **1995**, *145*, 293.

(29) Barone, V. *J. Chem. Phys.* **1994**, *101*, 6834.

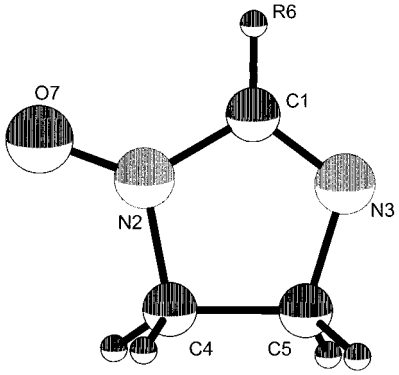


**Figure 1.** Schematic drawing and atom numbering of the iminonitroxide radical.

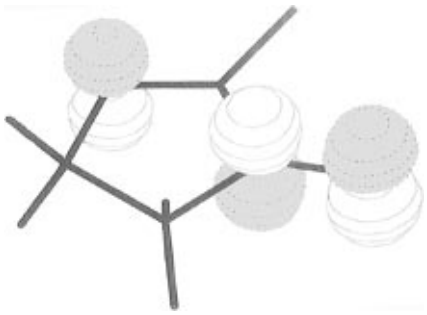

**Figure 2.** Schematic drawing of the frontier orbital (SOMO) for the iminonitroxide radical.

**Table 1.** Geometries Optimized by Different Quantum Mechanical Models for the Simple Iminonitroxide Radical ($R_6$ = H) Compared to Available Experimental Data from Refs 27 and 28[a]

| geometrical parameters | expt[b] | expt[c] | UHF/ 3-21G[d] | UHF/ 6-311G**[d] | B3LYP/ 6-31G* |
|---|---|---|---|---|---|
| $C_1H_6$ | | | 1.062 | 1.073 | 1.085 |
| $C_1N_2$ | 1.412 | 1.391 | 1.392 | 1.381 | 1.392 |
| $C_1N_3$ | 1.264 | 1.281 | 1.277 | 1.268 | 1.283 |
| $N_2C_4$ | 1.502 | 1.486 | 1.477 | 1.459 | 1.481 |
| $N_2O_7$ | 1.248 | 1.267 | 1.321 | 1.241 | 1.268 |
| $N_3C_5$ | 1.524 | 1.479 | 1.509 | 1.468 | 1.482 |
| $C_4C_5$ | 1.553 | 1.516 | 1.564 | 1.543 | 1.548 |
| $C_4H_9$ | | | 1.079 | 1.083 | |
| $N_3C_1N_2$ | 112.35 | 112.2 | 114.9 | 115.3 | 116.1 |
| $C_1N_2C_4$ | 111.6 | 109.7 | 110.4 | 109.4 | 108.5 |
| $C_1N_3C_5$ | 108.75 | 109.7 | 108.1 | 107.9 | 107.1 |
| $C_1N_2O_7$ | 125.95 | 125.2 | 124.8 | 125.8 | 126.6 |
| $N_2C_4C_5$ | 97.6 | 100.6 | 100.5 | 100.7 | 101.0 |
| $N_3C_5C_4$ | 106.25 | 105.9 | 106.1 | 106.7 | 107.3 |
| $N_2C_4H_9$ | | | 110.0 | 109.7 | |
| $N_3C_5H_{11}$ | | | 108.4 | 108.8 | |
| $H_6C_1N_2$ | | | 119.1 | 118.8 | 117.9 |
| $H_6C_1N_3$ | | | 126.0 | 125.9 | 125.9 |

[a] Bond lengths are in angstroms, and bond angles are in degrees. [b] $R_6 = C_6H_4NO_2$. [c] $R_6 = C_6H_5$. [d] From ref 25.

involving a formal ($N^+-O^-$) charge separation. The results are, however, not very different from those obtained for the isolated molecule.

In the same table, we show a comparison between the ASPs calculated at the UB3LYP and UHF levels, using the standard 6-31G* basis set. The considerable spin contamination of the UHF wave function ($S^2 = 0.92$) involves an overestimation of the spin polarization effect; in fact the UHF ASPs are significantly larger than experimental and B3LYP values. As previously noticed, ASPs are significantly reduced upon spin projection of the UHF wave function. The results remain, however, quite far from experimental and B3LYP values. Since CAS-SCF computations of biradicals are implicitly based on

**Table 2.** Experimental[28] and Theoretical Atomic Spin Populations for the Iminonitroxide Radical

| | | 6-31G*[b] | | | | EPR-II[b,d] | |
|---|---|---|---|---|---|---|---|
| atom | expt[a] | UHF | PUHF | B3LYP | EPR-II[b,d] | (water) | EPR-II[c,d] |
| $C_1$ | −0.057 | −0.553 | −0.167 | −0.133 | −0.123 | −0.133 | −0.104 |
| $N_2$ | 0.335 | 0.333 | 0.279 | 0.309 | 0.308 | 0.365 | 0.333 |
| $N_3$ | 0.236 | 0.587 | 0.302 | 0.292 | 0.285 | 0.293 | 0.287 |
| $C_4$ | 0.027 | −0.058 | −0.018 | −0.031 | −0.024 | −0.028 | −0.028 |
| $C_5$ | −0.027 | −0.063 | −0.021 | −0.017 | −0.016 | −0.016 | −0.017 |
| $H_6$ | | 0.035 | 0.012 | 0.004 | 0.004 | 0.004 | |
| $O_7$ | 0.407 | 0.640 | 0.577 | 0.511 | 0.507 | 0.448 | 0.486 |
| $H_8$ | | 0.021 | 0.011 | 0.022 | 0.020 | 0.022 | 0.021 |
| $H_9$ | | 0.021 | 0.011 | 0.022 | 0.020 | 0.022 | 0.021 |
| $H_{10}$ | | 0.018 | 0.007 | 0.009 | 0.010 | 0.011 | 0.010 |
| $H_{11}$ | | 0.018 | 0.007 | 0.009 | 0.010 | 0.011 | 0.010 |

[a] $R_6 = C_6H_4NO_2$. [b] $R_6$ = H. [c] $R_6 = C_6H_5$. [d] UB3LYP level.

restricted open Hartree−Fock (ROHF) computations for the constituting radicals, the contribution of spin polarization effects cannot be reliably estimated by these approaches. Taking into account that the excited configurations that improve the energy are often not the same as those that improve spin distributions, multireference configuration interaction approaches could also not be completely reliable in this connection, unless employing a prohibitive number of carefully selected configurations.

From an interpretative point of view, all methods agree in their indication that most of the spin density on the $N_2$, $N_3$, and $O_7$ atoms arises from spin delocalization (SD) effects and may be attributed to the unpaired electron in the singly occupied $\pi$ molecular orbital (SOMO).

On the $sp^2$ carbon atom $C_1$, a negative ASP is observed, originating, as pointed out by Zheludev et al.,[28] from a competition between spin polarization (SP) and SD. The contribution of $C_1$ AOs to the SOMO is rather small, and the SD and SP densities on $C_1$ are of the same order of magnitude, the latter being slightly larger thus leading to a small negative value for the complete spin population.

**(b) Geometrical Structure of Bis(imino)nitroxide.** In all computations, the methyl groups present in the socalled Ullman nitroxide biradical[30] have been replaced by hydrogen atoms. Thereafter, we will refer to this model as **C1** (Figure 3).

The conformational behavior of **C1** in its triplet state has been investigated by both UB3LYP and ROHF computational models using the FR approach discussed in the computational details. We have next computed an analogous potential energy profile for the singlet state using BS-B3LYP computations at the geometries optimized for the triplet state. Finally, the geometry of the cis structure ($\alpha = 0°$) of the singlet state has been fully optimized at the CAS(2,2) level.

The curves of Figure 4 show that triplet and singlet states have a very similar conformational behavior characterized by an energy minimum near $\alpha = 68°$ and a significant barrier for the *cis* conformation. While the general trends are similar by B3LYP and ROHF computations, the energy difference between the *cis* and minimum conformations is significantly smaller at the UB3LYP level. This is induced by the particular tendency of the UB3LYP approach, compared to that of ROHF, to stabilize conjugated systems, which is also apparent in some geometrical parameters. Therefore, for instance, the $C_1-C_6$ bond length obtained at the UB3LYP level is shorter than the corresponding ROHF value (see Table 3).

The geometrical parameters optimized at the ROHF and B3LYP levels for the planar and equilibrium structures of the triplet state are shown in Table 3. The general agreement

(30) Ullman, E. F.; Boocock, D. G. B. *J. Chem. Soc., Chem. Commun.* **1961**, 1161.

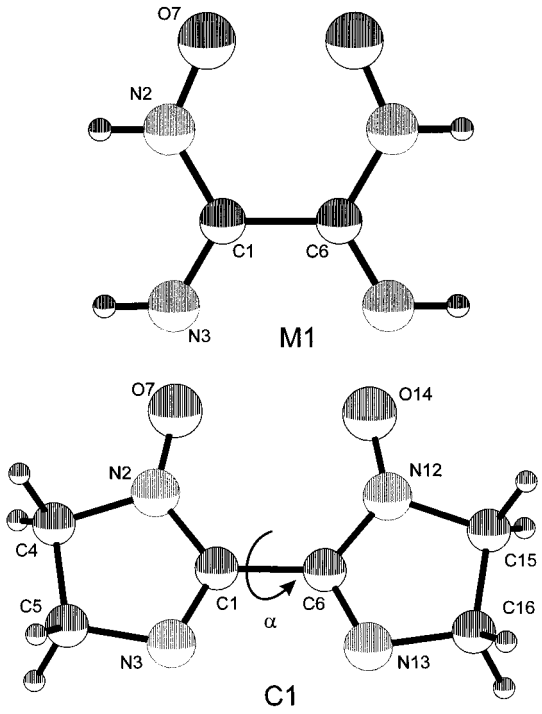


**Figure 3.** Schematic drawings and atom numberings of bis(imino)-nitroxide **C1** and its simplified model **M1**.

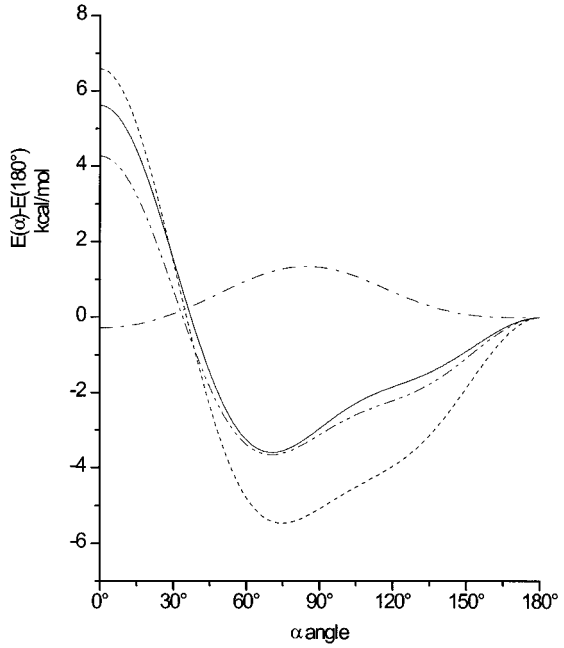


**Figure 4.** Potential energy profiles as a function of the α angle for bis(imino)nitroxide radical. Energy of the triplet state by UB3LYP (—) and ROHF (- - -) methods; energy of the singlet state by BS-B3LYP (— - -) model and solvation free energy of the triplet state by the PCM/UB3LYP model (— -). All of the terms are referred to values at $\alpha = 180°$.

between both computational models is quite apparent and suggests that significant geometry distortions (especially of CNO valence angles) occur for conformations near the *cis* one. As we shall see, this can have some impact on the magnetic coupling computed employing rigid geometries.

Another significant aspect is the close similarity between the structures obtained for the *cis* conformation of singlet (CAS results in Table 3) and triplet (ROHF results in Table 3) states. This shows that optimization of the triplet state, which can be efficiently done at the UB3LYP level, could be generally

**Table 3.** Geometries Optimized by Different Quantum Mechanical Models[a] for Bis(imino)nitroxide Compared to Available Experimental Data from Ref 15[b]

| | cis | | | minimum | | trans |
|---|---|---|---|---|---|---|
| geometrical parameters | CAS(2,2) (singlet) | ROHF (triplet) | B3LYP (triplet) | B3LYP (triplet) | expt | B3LYP (triplet) |
| $C_1C_6$ | 1.507 | 1.508 | 1.498 | 1.468 | 1.522 | 1.477 |
| $C_1N_2$ | 1.407 | 1.408 | 1.412 | 1.398 | 1.407 | 1.413 |
| $C_1N_3$ | 1.251 | 1.251 | 1.291 | 1.284 | 1.172 | 1.289 |
| $N_2C_4$ | 1.457 | 1.457 | 1.484 | 1.480 | 1.484 | 1.483 |
| $N_2O_7$ | 1.253 | 1.252 | 1.262 | 1.265 | 1.281 | 1.262 |
| $N_3C_5$ | 1.458 | 1.458 | 1.469 | 1.480 | 1.462 | 1.474 |
| $C_4C_5$ | 1.536 | 1.536 | 1.536 | 1.547 | 1.557 | 1.539 |
| $N_3C_1N_2$ | 113.5 | 113.5 | 114.0 | 115.9 | 116.2 | 114.7 |
| $C_1N_2C_4$ | 109.2 | 109.2 | 108.3 | 108.5 | 109.9 | 108.2 |
| $C_1N_3C_5$ | 109.9 | 109.9 | 108.9 | 107.2 | 109.1 | 108.2 |
| $C_1N_2O_7$ | 128.3 | 128.9 | 130.6 | 126.5 | 128.7 | 129.3 |
| $N_2C_4C_5$ | 101.0 | 101.0 | 101.9 | 101.1 | 96.79 | 101.6 |
| $N_3C_5C_4$ | 106.4 | 106.4 | 106.9 | 107.4 | 105.8 | 107.2 |
| $N_2C_1C_6$ | 127.8 | 127.9 | 127.5 | 118.6 | 114.1 | 120.8 |
| $N_3C_1C_6$ | 118.7 | 118.6 | 118.5 | 125.5 | 129.3 | 124.5 |
| $N_2C_1C_6N_{12}$ | | | | 68.04 | 63.59 | 180 |
| $N_3C_1C_6N_{13}$ | | | | 68.04 | 56.63 | 180 |
| $C_1C_6N_{12}C_{15}$ | | | | 180.0 | 172.3 | 180 |
| $C_1C_6N_{13}C_{16}$ | | | | 180.0 | 172.2 | 180 |
| $O_7N_2C_1C_6$ | | | | 0.0 | 1.890 | 0.0 |
| α | | | | 68.04 | 55.00 | 180.0 |

[a] All of the computations have been performed using the standard 6-31G* basis set. [b] Bond lengths are in angstroms, and valence bond angles are in degrees.

sufficient also for the singlet state (which would require a multiconfigurational treatment).

The geometrical parameters, calculated at the B3LYP/6-31G* level, for each ring of **C1** are very close to those obtained at the same level for the iminonitroxide radical. This confirms that when two aromatic rings are joined by a C—C bond, only the local environment of the inter-ring bond is modified when significant steric interactions are switched on (as in the *cis* conformation).

We can also compare the geometrical parameters obtained by UB3LYP/6-31G* computations with X-ray data.[15] The experimental structure indicates a slight distortion of each ring from planarity, which has been related to the presence in the unitary cell of two different molecules that are statistically disordered because of the effect of crystal packing.

A consequence of distortion from planarity is that the dihedral angles $N_2C_1C_6N_{12}$ and $N_3C_1C_6N_{13}$ are different from each other and from the angle between the average planes of the two rings ($\alpha = 55°$).[15]

In any case, the computed geometrical parameters are close to experimental data, except for those for the $C_1—N_3$ bond length. It should be noticed, in this connection, that the X-ray value for the anologous bond in the second ring is considerably different (1.172 Å versus 1.391 Å), thus suggesting that the theoretical result could be more reliable.

In the same table are shown the bond lengths and the valence angles optimized at the B3LYP/6-31G* level for the *trans* conformation of **C1**. It is noteworthy that all geometrical parameters are close to those of the equilibrium conformation, but some of them are quite different from those of the *cis* structure. Since this is also the case for the other optimized structures used for FRM computations, we can conclude that only cisoid conformers require specific geometry optimization in view of close contacts between the NO groups belonging to different rings.

We have next computed the modifications induced in the torsional potential of **C1** by the chloroform solvent. The solvation free energy, shown in Figure 4, has a trend opposite to

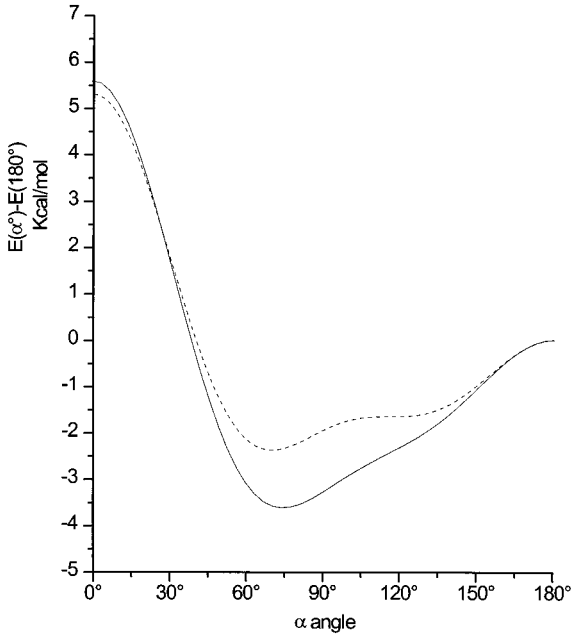


**Figure 5.** Torsional energy in vacuo (—) and total free energy in chloroform (- - -) as a function of the α angle computed for the triplet state of bis(imino)nitroxide at the B3LYP/6-31G* level. Both terms are referred to values at α = 180°.

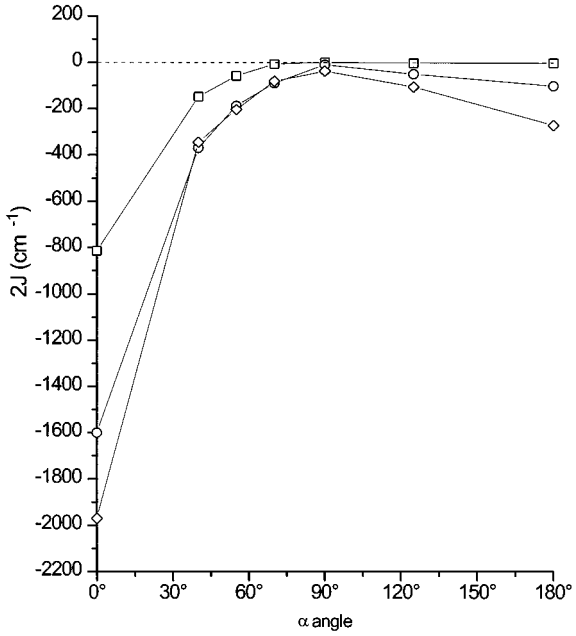


**Figure 6.** Comparison between the singlet−triplet gap as a function of the conformational angle α in the model compound **M1** obtained by CAS(2,2) (□), BS-B3LYP (◇), and dedicated CI (○, from ref 31) approaches.

that of the intrinsic torsional energy in that planar or nearly planar structures are now preferred with respect to the twisted minimum obtained in vacuo. As a consequence, the optimized equilibrium torsional angle is smaller in condensed phases than in vacuo (see Figure 5), the effect increasing with the polarity of the environment. In particular the value optimized in chloroform (60°) is remarkably close to the experimental value in the solid state (55°).

An interesting point which emerges from Figure 4 is that the solvation energies of *cis* (α = 0°) and *trans* (α = 180°) conformations are similar to each other, although they have very different dipole moments (1.67 D in the first and 0 D in the second). This implies that a simple continuum model of solvation, in which the multipolar development of solute−solvent interactions is truncated at the dipole level (the Onsager model), cannot be used.

**(c) Magnetic Coupling in Bis(imino)nitroxide Radicals.** In order to validate the B3LYP approach for the computation of magnetic couplings of different strengths, we have used the simplified **M1** model shown in Figure 3 for which very refined computations are available for different conformations spanning a range of magnetic couplings between 0 and 2000 $cm^{-1}$ (see Figure 6). Since individual geometric parameters are not reported in ref 31, we have followed the same strategy, using the experimental geometrical data of ref 25, except for the C−C distance, which has been taken from ref 15, and the N−C−C valence angle, which has been obtained bisecting the supplementary of the internal N−C−N angle.

The B3LYP values agree with those computed in ref 31 using specific CI calculations in the whole torsional space. The singlet−triplet (S−T) gap is much smaller in the *trans* than in the *cis* conformation, because in the first case the distance between magnetic groups is large and through-space interactions are smaller than in the second case. For α = 0° the S−T gap computed at the BS-B3LYP level is larger than that reported in ref 31. This could, however, be due to different values of C−N−O angles used in the two computations. As a matter of fact, a rough investigation at the CAS-SCF(2,2) level indicates that variations of 10° in the C−N−O angles involve variations as large as 2000 $cm^{-1}$ in the S−T gap. This is due to the well-known exponential variation of the S−T gap with the distance between the magnetic centers.[32] This observation indicates that for molecules with strong couplings between their magnetic subunits reliable results can only been obtained after careful geometry optimizations.

The small magnitude of the S−T separation in perpendicular or nearly perpendicular conformations is due to the near orthogonality of the magnetic orbitals. In this case BS-B3LYP and dedicated CI results are in good agreement.

CAS-SCF(2,2) calculations have been also performed. The computed S−T splittings are smaller than those obtained by the BS-B3LYP approach especially in the region of strong interactions and can be considered at most in qualitative agreement with experimental data. Extension of the active space by a CAS(6,6) computation does not rectify matters, thus showing that only extensive inclusion of dynamic correlation can lead to reasonable results.

We have next performed an analogous study for the **C1** molecule, whose $\pi$ magnetic orbitals are shown in Figure 7.

In Figure 8, we show a comparison between the magnetic interactions computed for the biradicals **M1** and **C1**.

It is quite apparent that the influence of the substituents external to the region of the interaction between the radical fragments, i.e., the methylene groups of each monomer, does not affect significantly the magnitude of the S−T gap and its behavior as a function of the α angle. This gives further support to the results of ref 31, except for the already mentioned dependence on geometry optimization for crowded conformations, such as the cis one.

We have also considered solvent effects on the computed S−T gap, but the results are only slightly affected by this contribution, at least for solvents that are not too polar. Of course, indirect solvent effects are not negligible, since even small solvent-induced modifications of the equilibrium α angle

(31) Castell, O.; Caballol, R.; Subra, R.; Grand, A. *J. Phys. Chem.* **1995**, *99*, 154.

(32) Yaughuchi, K.; Okumura, M.; Mori, W.; Maki, J.; Takda, K.; Noro, T.; Tanaka, K. C*hem. Phys. Lett.* **1993**, *210*, 201.

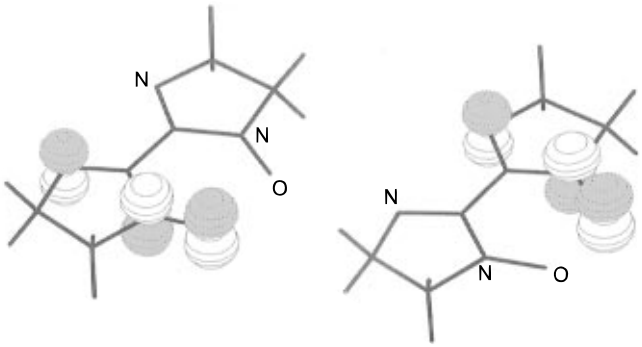


**Figure 7.** Schematic drawings of the $\pi$ magnetic orbitals obtained for bis(imino)nitroxide by BS-B3LYP computations.

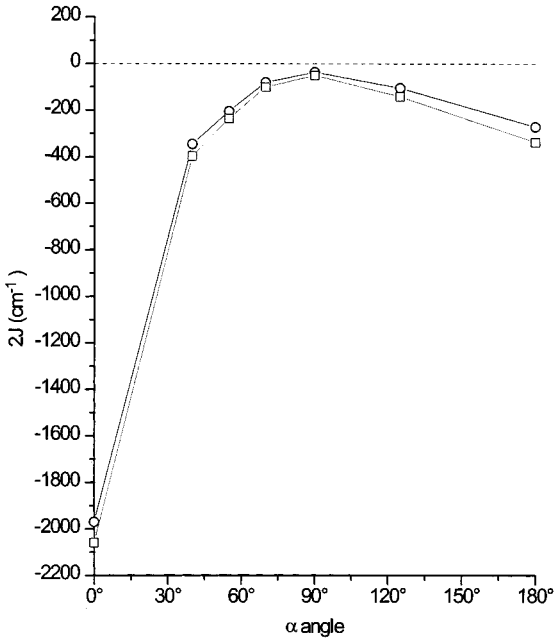


**Figure 8.** Comparison between the variation of the singlet−triplet gap as a function of the torsional angle α obtained for **C1** (□) and **M1** (○) models by BS-B3LYP computations.

lead to significant changes of the magnetic coupling. This points out, once again, the significance of a comprehensive computational protocol able to take into the proper account electronic, geometrical, and environmental effects at the same level and for quite large systems.

As a final point, we compared the magnetic couplings obtained by different methods for the **C1** biradical at the experimental torsional angle ($\alpha = 55°$). The results in Table 4 show that all of the density functional approaches provide reasonable magnetic couplings.

From a more quantitative point of view, the value obtained by local functionals (−128 and −150 $cm^{-1}$ at the Xα and SVWN levels, respectively) is decreased including gradient corrections (−128 $cm^{-1}$ at the BLYP level) and is lead into close agreement with experiment only when adding also some exact exchange (−212 $cm^{-1}$ at the B3LYP level). At the same time, the detailed form of the correlation functional plays only a minor role, since B3LYP and B3PW91 results are very close (−212 and −214 $cm^{-1}$, respectively). The gap obtained by these functionals is in remarkable agreement both with the most refined post-HF computations (208 $cm^{-1}$)[31] and with experiment.

**Table 4.** Energy Gaps between Singlet and Triplet States of Bis(imino)nitroxide Obtained by Different Methods at $\alpha = 55°$ Compared to Those Measured in Condensed Phases

| methods | 2J ($cm^{-1}$) |
|---|---|
| BS-Xα | −122 |
| BS-B3LYP | −212 |
| BS-B3PW91 | −214 |
| BS-BLYP | −128 |
| BS-SVWN | −151 |
| BS-SVWN5 | −153 |
| dedicated CI | −209[a] |
| expt[b] | −194[c], −163[d] |

[a] From ref 31. [b] From ref 15. [c] Solid state. [d] Mixture of chloroform/methylene.

Also taking into account that the B3LYP model significantly improves the reliability of standard density functional models concerning geometric, thermodynamic, and spectroscopic parameters,[8] we believe that the further computational effort implicit in this kind of hybrid density functional/Hartree−Fock approaches is well compensated by their increased reliability and large field of application.

## Conclusions

A powerful density functional/Hartree−Fock hybrid (the B3LYP model) has been used to investigate structural and magnetic properties of a prototypical stable free radical and of the biradical obtained joining two identical units. Moreover solvent effects have been taken into account by a reliable continuum solvent model (PCM).

Comparison with experiment shows that the geometry and spin distribution of iminonitroxide are well reproduced by our approach, as is also the case for the magnetic coupling of bis(imino)nitroxide. Furthermore, our results for a simplified model of the biradical are in good agreement with previous refined computations for the whole range of values obtained by varying the torsional angle between the two iminonitroxide units.

A full geometry optimization for the triplet electronic state points out some inconsistencies in the available X-ray values. Furthermore, a parallel CAS-SCF computation indicates that the geometrical parameters of the singlet and triplet states are very close. However, this kind of computations provide reliable magnetic couplings only for weak interactions between the radical moieties.

Although solvent effects on the magnetic coupling are negligible, they modify the torsional potential for rotation around the inter-ring bond, bringing the equilibrium dihedral angle into better agreement with the experimental value in the solid state.

In summary, the combined use of hybrid density functional/Hartree−Fock methods and refined continuum solvent models paves the route for the investigation of large magnetic systems in solution. This becomes increasingly more valid as promising results are also being obtained for molecular magnets including transition metal atoms,[33,34] and the whole computational protocol is or will be shortly available to other researchers in the field through standard quantum chemistry packages.

JA9709785

(33) Ruiz, E.; Alemany, P.; Alvarez, S.; Cano, J. *J. Am. Chem. Soc.* **1997**, *119*, 1297.

(34) Bencini, A.; Totti, F.; Daul, C.; Doclo, K.; Fantucci, P.; Barone, V. *Inorg. Chem.* In press.